Eur. Pharm. J. 2026, AoP.
ISSN 1338-6786 (online) and ISSN 2453-6725 (print version),
DOI: 10.2478/afpuc-2026-0002

EUROPEAN PHARMACEUTICAL JOURNAL

Response Surface Methodology-Guided Optimization of Flucytosine Nanoemulsion for Enhanced Antifungal Performance

Research paper

Priya Tiwari✉, Shipra Verma, Gajendra Saini

MET: Moradabad Educational Trust Group of Institutions Moradabad, Uttar Pradesh INDIA

Received 22 August, 2024, accepted 8 October, 2024

Abstract Although flucytosine is a powerful antifungal drug, formulation-related issues frequently restrict its clinical usage, and the growing prevalence of invasive fungal infections caused by *Candida* and *Cryptococcus* species poses a serious public health problem. This work designed, optimized, and assessed a flucytosine-loaded nanoemulsion using a Box–Behnken experimental design to improve physicochemical stability and antifungal activity. Pre-formulation studies confirmed the purity, crystallinity, and compatibility of flucytosine with selected excipients. A total of 17 nanoemulsion formulations were prepared by varying the oil concentration, surfactant–co-surfactant (Smix) ratio, and homogenization time, with particle size, polydispersity index (PDI), and entrapment efficiency (%EE) as key responses. The optimized formulation (F7) exhibited a small droplet size (~104 nm), low PDI (<0.3), high entrapment efficiency (~95%), suitable pH, and a stable negative zeta potential, indicating excellent physical stability. Transmission electron microscopy confirmed spherical and uniformly dispersed droplets. In vitro drug release studies demonstrated a sustained release profile over 24 hours, with the optimized formulation showing significantly higher cumulative drug release compared to other batches. Antifungal evaluation against *Candida albicans* revealed a markedly larger zone of inhibition for the nanoemulsion compared to plain drug solution, indicating enhanced antifungal efficacy. Stability studies conducted under International Council for Harmonisation (ICH) conditions confirmed the formulation's stability over 3 months. Overall, the proposed flucytosine nanoemulsion demonstrated higher antifungal activity, prolonged drug release, better physicochemical features, and good stability, suggesting its potential as a successful antifungal therapeutic delivery method.

Keywords *Flucytosine – Nanoemulsion – Antifungal Activity – Candida albicans – Drug Delivery System – Stability Studies*

INTRODUCTION

A major public health concern is the rise of pathogenic fungi that can infect humans. Topical and oral drugs are routinely used to treat fungal illnesses like blastomycosis and histoplasmosis. However, oral drugs are less effective due to their low absorption (Denning, 2024; Linder et al., 2023; Liu et al., 2025). For many years, the treatment of severe fungal infections has relied heavily on flucytosine, an antifungal drug with strong action against *Cryptococcus* and *Candida* species (Sigera & Denning, 2023). Despite its effectiveness, flucytosine is still not widely available in many areas, which prevents it from being widely used to treat invasive fungal illnesses (Miot et al., 2021). Flucytosine's synergistic effect in combination therapy, especially with amphotericin B, has demonstrated encouraging outcomes in lowering mortality in Candida meningitis and increasing survival rates in cryptococcal meningitis, highlighting its critical role in treating these potentially fatal infections (Hurt et al., 2021; Jarvis et al., 2022). To lessen the effects of invasive fungal diseases, however, obstacles including the development of resistance during monotherapy for some fungal infections highlight the significance of additional research and initiatives to improve access to flucytosine, particularly in low-income nations (Miot et al., 2021).

Fungal DNA and RNA synthesis is inhibited by flucytosine, an antifungal drug that works against *Cryptococcus* and *Candida* species (Delma et al., 2021).

This method impedes the metabolism of nucleic acids, which impairs the creation of proteins and ultimately causes fungal cells to die. Flucytosine can readily penetrate the eye, urinary tract, central nervous system, and cardiac vegetations because of its high water solubility. Its efficacy in treating fungal infections is increased by this capability. Flucytosine

* *E-mail: tiwari93priya@gmail.com*

exhibits early fungicidal effectiveness against *Cryptococcus* species when combined with amphotericin B, improving survival rates in cases of cryptococcal meningitis. Flucytosine's synergistic action with amphotericin B has been especially helpful in lowering mortality in neonatal candidiasis and Candida meningitis, highlighting its significance in severe fungal infections (Delma et al., 2021; McHale et al., 2023; Sigera & Denning, 2023).

After being absorbed by susceptible fungal cells, flucytosine is converted into 5-fluorouracil (5-FU), which then inhibits the production of fungal DNA and RNA. Flucytosine is well absorbed, effectively penetrates body tissues, and is mainly excreted by the kidneys after oral treatment (Sastré-Velásquez et al., 2022; Sigera & Denning, 2023).

Surfactants, which are surface-active compounds, stabilize nanoemulsions (NEs), which are complex mixtures of two immiscible liquids, typically water and oil (Shaker et al., 2019). Through their adsorption at the oil–water interface, surfactants lessen the chance of coalescence, which lowers surface tension and contributes to emulsification.

By forming a film at the oil–water interface and slowing down destabilization processes, surfactants help separate or disrupt dispersed phases. The formation of NEs with certain physicochemical properties depends on the choice of surfactants. NEs are thermodynamically unstable yet kinetically stable due to their droplet sizes, which fall between 10 and 1000 nm (Nikolaev et al., 2023). This instability arises from the increased free energy present in the system compared to the individual phases (Tayeb et al., 2021).

Experimental design is commonly used to optimize nanoparticles due to its benefits, including reducing the number of experiments required, creating mathematical models to evaluate the importance and statistical significance of factor effects, and assessing the interaction effects between factors (Rampado & Peer, 2023). Statistical experimental design approaches are widely employed in nanoparticle optimization due to their ability to reduce experimental runs while providing comprehensive evaluation of formulation variables and their interactions. The Box–Behnken design (BBD), a response surface methodology based on a three-level incomplete factorial design, is particularly effective for optimizing pharmaceutical formulations while avoiding extreme experimental conditions.

Therefore, the present study aimed to design, develop, and optimize a flucytosine-loaded nanoemulsion using the Box–Behnken design to enhance its physicochemical characteristics and therapeutic potential for the effective management of fungal infections.

MATERIAL AND METHOD

Flucytosine, API grade, was acquired from Yarrow Chem Products, Mumbai, India. Liquid paraffin and Propylene glycol were purchased from S. K. Scientific Instruments Pvt. Ltd., U.P., India. Tween-80 was purchased from Tomar Scientific Corporation, Rajasthan, India. All other chemicals were of analytical reagent grade and used as received without further purification.

Methods

Pre-formulation studies

Physical Appearance

Physical appearance evaluation was carried out for the pure drug (flucytosine) and selected excipients (liquid paraffin, Tween-80, and propylene glycol) based on observable characteristics such as color, odor, and texture (Clapham et al., 2023).

Solubility Studies

The solubility of flucytosine in various solvents was evaluated using a semi-quantitative shake–vortex method. Briefly, 10 mg of drug was added to 2 mL of each solvent and subjected to vortex mixing (2500 rpm, 5 min) followed by agitation for 30 min at 25 ± 2 °C. Samples were visually inspected for undissolved particles. If complete dissolution was not achieved, additional solvent was added incrementally until a clear solution was obtained. Solubility was classified semi-quantitatively based on the extent of dissolution and the approximate solvent volume required for complete solubilization, as freely soluble, soluble, sparingly soluble, slightly soluble, or practically insoluble (Cong et al., 2021).

Melting Point

The established criteria evaluate the purity of the active pharmaceutical ingredient (API), among other quality attributes. The melting point of pure synthetic compounds is typically constant and sharp. Drugs may exhibit a specific melting point range because they often consist of mixed synthetic ingredients. A little quantity of powder is attached to a tube. The fusion tube was placed in a castor oil-filled melting point determining equipment (Chemline). The temperature of the castor oil gradually increased, the temperature at which the powder started to soften, and the temperature after the powder has completely melted are all taken into account (Yalkowsky & Alantary, 2018).

Spectrophotometric Analysis of Flucytosine

An accurately weighed quantity of flucytosine (100 mg) was dissolved in 100 mL of 0.1 N hydrochloric acid to obtain a stock solution (1000 µg/mL). A suitable aliquot was further diluted with the same solvent to prepare the working solution. The UV absorption spectrum was recorded using a UV-Visible spectrophotometer (UV-1900i, Shimadzu, Japan) over the

wavelength range of 200–400 nm, and the absorption maximum (λ_{max}) was determined (Kamdi et al., 2020).

Drug-Excipient Compatibility Study by Fourier Transform Infra-Red (FTIR) Spectroscopy

FTIR analysis of flucytosine was performed using a PerkinElmer Spectrum IR spectrophotometer (version 10.7.2) to identify characteristic functional groups. Samples were prepared using the potassium bromide pellet method by mixing approximately 10 mg of flucytosine with dry potassium bromide under high compression. The spectra were recorded over the range of 4000–400 cm^{-1} after baseline correction (Tkachenko & Niedzielski, 2022). Drug stability and bioavailability may be impacted by any chemical or physical interactions with excipients. We made a tiny 1:1 blend of medications and excipients. The mixture was put in vials above. The vials were sealed hermetically with rubber seals. After 4 weeks of storage at room temperature, the drug-excipient compatibility was examined. The FTIR method was also used to test the samples (Patel et al., 2015).

X-ray diffraction (XRD) study

XRD analysis was conducted to determine the crystalline nature of flucytosine using an X-ray diffractometer. Diffraction patterns were recorded over a 2θ range of 0–80°, and the intensity of diffraction peaks was analyzed to assess crystallinity (Ali et al., 2022).

Formulation Development

Preparation of Nanoemulsion as per the Experimental Design

The Box–Behnken design (BBD) is a well-recognized and commonly adopted method for optimizing nanoemulsion formation. The implementation and interpretation of this method involve experimental techniques, which were compared to other approved ways (Beg et al., 2012). The Box–Behnken design (BBD) was employed to optimize the formulation variables influencing nanoemulsion characteristics. Three independent variables were selected: amount of oil (X_1), surfactant–co-surfactant mixture (S_{mix}) ratio (X_2), and homogenization time (X_3). Particle size (Y_1), polydispersity index (PDI) (Y_2), and entrapment efficiency (%EE) (Y_3) were selected as dependent responses.

The experimental design comprised 17 runs, including replicated center points, and data analysis was performed using Design-Expert® software (version 12.0.3.0, Stat-Ease Inc., Minneapolis, MN, USA). A quadratic polynomial model was applied to evaluate the effects of formulation variables and their interactions.

Table 1. Variables in Box–Behnken design

Factor Independent variables	Levels used		
	-1	0	+1
Amount of oil (mL) (X1)	5	10	15
S_{mix} (X2)	1.0	1.5	2.0
Homogenization Time (min) (X3)	20	25	30
Dependent variables	**Constraints**		
Particle size (nm) (Y1)	Minimize		
PDI (Y2)	Minimize		
Entrapment Efficiency (%) (Y3)	Maximize		

Preparation of Nanoemulsion

The flucytosine nanoemulsion was created using a high-speed homogenizer (JHG-54-P100, Shanghai Pulisheng Fusion Machinery Co., Ltd., China) (Shi et al., 2022). Accurately weighed flucytosine (100 mg) was first dissolved in the oil phase in a clean, dry beaker with gentle magnetic stirring to ensure complete drug solubilization. Tween 80 (surfactant) and propylene glycol (co-surfactant) were mixed separately in the specified S_{mix} ratios to obtain a homogeneous S_{mix} blend. The prepared S_{mix} was then added gradually to the oil–drug mixture under continuous stirring until a clear and uniform preconcentrate was obtained. Subsequently, the required quantity of distilled water was added dropwise to the mixture with constant stirring at a moderate speed. The system spontaneously formed a transparent or slightly bluish nanoemulsion upon aqueous dilution. The final nanoemulsion was stirred for an additional 15–20 minutes at 15,000 rpm to ensure uniformity and stability.

The resulting nanoemulsion was then sonicated for 10 minutes using the probe sonication technique to make sure the nanoemulsion was created, and all the contents were well combined, shown in Table 2 (Khani et al., 2016).

Characterization of Nanoemulsion

Particle Size Distribution

The Zetasizer Ver 7.13 (Malvern Instruments, Ltd., UK) was used to measure the size of the nanoemulsion particles three times. A cuvette was filled with an aliquot of around 1 ml. Using a light scattering angle of 90°, the mean particle diameter and polydispersity index (PDI) were calculated at a temperature of 25±2°C. The degree of homogeneity and distribution of the globules were assessed using the polydispersity index (PDI). Monodispersity was considered to be indicated by a PDI score of less than 0.3 (Anwer et al., 2023).

Table 2. Composition and observed responses in Box–Behnken design

Batch	Drug (mg)	Independent Variables			Dependent variables		
		A:Amount of Oil (ml) (X1)	Smix (X2)	Homogenization Time (min) (X3)	Particle Size (nm)	PDI	%EE
1	100	5	1.5	30	269	0.141	79.81
2	100	10	1	30	224	0.106	96.01
3	100	5	1.5	20	278	0.133	71.12
4	100	10	1.5	25	229	0.112	85.89
5	100	5	2	25	257	0.148	71.89
6	100	5	1	25	271	0.141	72.45
7	100	15	1	25	202	0.117	84.31
8	100	15	1.5	20	203	0.105	86.93
9	100	15	2	25	197	0.116	89.18
10	100	10	1	20	219	0.119	91.43
11	100	10	2	30	218	0.121	92.87
12	100	10	1.5	25	215	0.112	82.16
13	100	15	1.5	30	198	0.109	84.57
14	100	10	2	20	211	0.104	90.79
15	100	10	1.5	25	222	0.115	87.11
16	100	10	1.5	25	217	0.111	84.94
17	100	10	1.5	25	212	0.11	86.91

Zeta potential

By identifying the electric charges on the globules' surface, zeta potential measurements were utilized to assess the degree of attraction and repulsion between NEs globules. Each formulation's zeta potential was assessed using a Malvern Zetasizer (Malvern Instruments, Worcestershire, UK). At a temperature of 25±2°C, the sample was diluted with distilled water in amounts ranging from 50 µl to 10 ml (Rasmussen et al., 2020).

pH and Conductivity Determination

A pH meter (EUTECH Instruments, Singapore) was used to measure the nanoemulsion compositions' pH at 25±2°C. To assure accuracy, the measurements were made three times. An electric current was run through a 20-ml sample of the formulation at 25±2°C to determine the nanoemulsion's conductivity. A conductivity meter (Model No. DB-1038, made by Decibel in India) with Pt/platinized electrodes was used for the experiment three times (Kumar et al., 2016).

% Entrapment efficiency (%EE)

The amount of unbound flucytosine in the dispersed aqueous phase was used to quantify the trapping efficiency of the flucytosine nanoemulsion. In summary, a cooling centrifuge made by REMI Instruments Ltd., India, was used to centrifuge a 2-ml sample of flucytosine nanoemulsion dispersion in an Eppendorf tube for 20 minutes at a speed of 12,000 rpm. The temperature at which the centrifugation was performed was 4°C. The liquid that remained after centrifugation was filtered after being suitably diluted with methanol. Next, flucytosine was measured at a wavelength of 285 nm using UV spectroscopy (Goyal et al., 2015). The following formula was used to calculate the entrapment efficiency percentage:

$$\%EE = \frac{\text{Totel quantity of flucytosine} - \text{Free quantity of flucytosine in supernatant}}{\text{Total quantity of flucytosine}} \times 100 \quad (1)$$

Drug Content

A volumetric flask was filled with a precisely measured volume of the flucytosine nanoemulsion, which is comparable to a known quantity of medication. To break up the emulsion and fully extract the medication, the nanoemulsion was diluted with an appropriate solvent, such as distilled water or methanol. The mixture was filtered through a 0.45-µm membrane filter to exclude any undissolved excipients after being sonicated for 10–15 minutes to guarantee full release of flucytosine from the formulation. A UV-visible spectrophotometer was used to measure the filtered solution at the predefined λmax of flucytosine after it had been appropriately diluted. A previously created flucytosine

calibration curve was used to determine the medication content (Safhi et al., 2023).

Morphology study by transmission electron microscopy (TEM)

TEM was used to analyze the morphology of the nanoemulsion, which was a useful technique for confirming the particle size. On perform transmission electron microscopy (TEM), a little amount of nanoemulsion was put on wax paper. The next stage was transforming the nanoemulsion onto a circular copper film matrix with a mesh size of 300. The sample was stained with a 2% w/v solution of phosphotungstic acid and then allowed to dry in ambient air. The morphology and dimensions of the air-dried grid were analyzed at 70 kV using a Morgagni 268D transmission electron microscope (FEI, Hillsboro, OR, USA) (Pangeni et al., 2014).

In Vitro Drug Release

In vitro drug release of the optimized flucytosine nanoemulsion was evaluated using the dialysis bag diffusion technique. A dialysis membrane with a molecular weight cut-off of 12–14 kDa was soaked overnight in distilled water prior to use. An accurately measured quantity of nanoemulsion equivalent to 10 mg of flucytosine was placed into the dialysis membrane, and both ends were securely tied to prevent leakage. The dialysis bag was immersed in 900 mL of phosphate buffer pH 6.8 as the release medium, maintained at 37 ± 0.5°C and stirred continuously at 100 rpm using a magnetic stirrer to simulate physiological conditions. At predetermined time intervals (0.5, 1, 2, 4, 6, 8, 12, and 24 h), 5 ml of the release medium was withdrawn and replaced with an equal volume of fresh buffer to maintain sink conditions. The collected samples were analyzed spectrophotometrically at the predetermined λmax of flucytosine after suitable dilution. The cumulative percentage of drug released was calculated and plotted against time to obtain the release profile (Vishwas et al., 2024).

Release kinetics

To better understand the mechanism of drug release from the optimized nanoemulsion formulation (F7), the in vitro release data were fitted to different kinetic models including zero-order, first-order, Higuchi, and Korsmeyer-Peppas models.
The mathematical equations used were:

Zero-order model

$$Q_t = Q_0 + k_0 t$$

where Q_t is the amount of drug released at time t, Q_0 is the initial amount of drug, and k_0 is the zero-order release constant.

First-order model

$$\log Q_t = \log Q_0 - \frac{k_1 t}{2.303}$$

where k_1 is the first-order release constant.

Higuchi model

$$Q_t = k_H \sqrt{t}$$

where k_H represents the Higuchi dissolution constant.

Korsmeyer–Peppas model

$$\frac{M_t}{M_\infty} = kt^n$$

where M_t/M_∞ is the fraction of drug released at time t, k is the release rate constant, and n is the release exponent indicating the drug release mechanism.

Antifungal Activity by Zone of Inhibition Method

The agar well diffusion (zone of inhibition) technique was used to assess the flucytosine nanoemulsion's antifungal efficacy against *Candida albicans*. Freshly produced fungal colonies were suspended in sterile saline, and the turbidity was adjusted to match the 0.5 McFarland standard (≈1–2 × 10^8 CFU/mL) to provide a standardized inoculum of *Candida albicans*. To ensure an equitable dispersion, sterile Sabouraud Dextrose Agar (SDA) plates were prepared and evenly infected with the fungal solution using a sterile cotton swab. A sterile cork borer was used to aseptically punch wells of consistent diameter (6–8 mm) into the agar. The flucytosine nanoemulsion was carefully added to the wells in a predetermined volume. A blank nanoemulsion was utilized as a negative control, and plain drug solution (flucytosine solution) was employed as a control. After allowing the samples to pre-diffuse for an hour at room temperature, the plates were incubated for 24 to 48 hours at 37 ± 2 °C. The plates were inspected for distinct zones of inhibition surrounding the wells following incubation. A digital caliper or calibrated ruler was used to measure the zones of inhibition's diameter in millimeters. By contrasting the nanoemulsion's zone sizes with those of the control and plain drug formulations, the antifungal efficacy was evaluated (Rai, M., Ingle, A. P., & Pandit, 2021).

Stability Studies

Stability studies of the flucytosine nanoemulsion were carried out in accordance with International Council for Harmonisation (ICH) guidelines to evaluate the physical and chemical stability of the formulation. The optimized nanoemulsion formulation was filled into tightly closed, amber-colored glass containers to protect it from light. The samples were stored under different conditions, namely refrigerated conditions (4 ± 2 °C), room temperature (25 ± 2 °C / 60 ± 5% RH), and accelerated conditions (40 ± 2 °C / 75 ± 5% RH). At predetermined intervals (0, 1, 2, and 3 months), samples were withdrawn and evaluated for changes in physical appearance (clarity, phase separation, creaming or cracking), pH, particle size and polydispersity index (PDI), zeta potential, and drug content/entrapment efficiency (Jacob et al., 2024).

Statistical Analysis

Statistical analysis was performed using GraphPad Prism (Version 10.6.0). The data are expressed as mean ± standard deviation (SD) from n = 3. The data analysis was conducted using one-way ANOVA, followed by the Tukey multiple comparison test to evaluate the experimental groups, with $P < 0.05$ deemed statistically significant across the groups.

RESULT AND DISCUSSION

Pre-formulation studies

Physical Appearances

Based on observable traits including appearance, texture, and odor, the physical evaluation of flucytosine revealed no odd or undesirable qualities. These findings imply that the physical characteristics of the drug are in line with accepted standards for pharmaceutical quality. All things considered, the acceptable sensory qualities support its appropriateness for patient usage and handling without posing stability or compliance issues.

Solubility Studies

In distilled water, 0.1 N hydrochloric acid, and phosphate buffer solutions at pH 5.5 and 6.8, flucytosine quickly and completely dissolved, demonstrating its free solubility in various aqueous media. The medication was categorized as soluble in phosphate buffer pH 7.4 and methanol because it entirely dissolved but needed a substantial amount of solvent. Ethanol was found to be sparingly soluble due to partial dissolution, which required a greater solvent volume. Acetone showed very little dissolving, suggesting extremely minor solubility, but propylene glycol only demonstrated limited dissolution, showing slight solubility. Flucytosine is essentially insoluble in non-polar organic solvents such as chloroform, diethyl ether, and hexane, which is attributed to its highly polar pyrimidine structure and strong hydrogen-bonding interactions with aqueous media rather than non-polar environments (Cong et al., 2021).

Melting Point

The melting point of flucytosine was determined using the fusion tube method with a Chemline melting point apparatus and castor oil as the heating medium. The sample began to soften at 296 °C and completely melted at 300 °C, indicating a melting point range of 296–300 °C. The observed melting range of flucytosine is consistent with pharmacopoeial standards, which report a melting point of approximately 295–300 °C (with decomposition), confirming the purity and identity of the drug (Monograph, 2014). The narrow melting range obtained in this experiment suggests that the flucytosine sample is relatively pure and meets established quality criteria.

UV-visible Spectroscopy

Absorption maxima (λ_{max}) of the flucytosine was conducted in 0.1N hydrochloric acid. It was found to be 285nm, as shown in Figure 1.

Drug–Excipient Compatibility Study by Fourier Transform Infra-Red (FTIR) Spectroscopy

The FTIR spectrum of flucytosine displayed distinctive absorption bands that validate its functional groups and structural integrity. A broad band at approximately 3300–3400 cm^{-1} correlates to N–H stretching, while peaks around 3000 cm^{-1} are ascribed to C–H stretching vibrations. Prominent bands in the 1650–1550 cm^{-1} range signify C=O stretching and N–H bending, denoting the existence of the pyrimidine ring. Peaks within the range of 1200–1000 cm^{-1} belong to C–N stretching, while bands below 800 cm^{-1} are linked to ring deformation and C–F stretching. The existence of these distinctive peaks validates the authenticity and purity of flucytosine. The typical drug peaks in the spectra of flucytosine with propylene glycol and Tween 80 were preserved. A broad band at around 3400–3450 cm^{-1} signifies the overlap of O–H stretching from the excipients with N–H stretching from flucytosine, implying potential hydrogen bonding. Peaks at around 2920–2930 cm^{-1} indicate aliphatic C–H stretching, although the typical C=O peak of the drug (~1650–1653 cm^{-1}) remained constant. Minor peak broadening was detected as a result of physical mixing. The lack of new peaks or notable changes signifies the absence of chemical interaction, hence affirming the compatibility of flucytosine with propylene glycol and Tween 80 for formulation development, as shown in Figure 2.

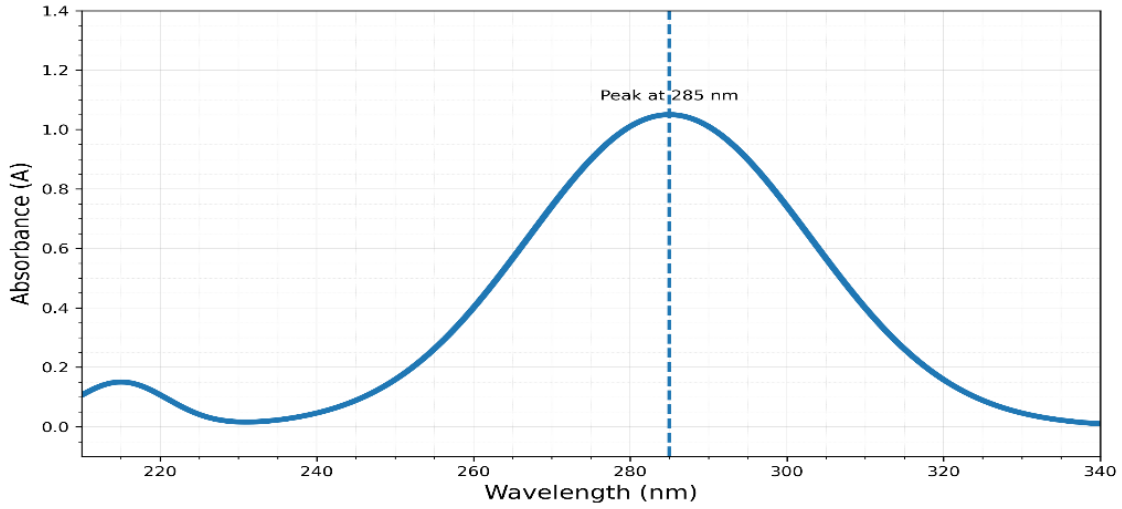

Figure 1. UV Spectrum of Flucytosine

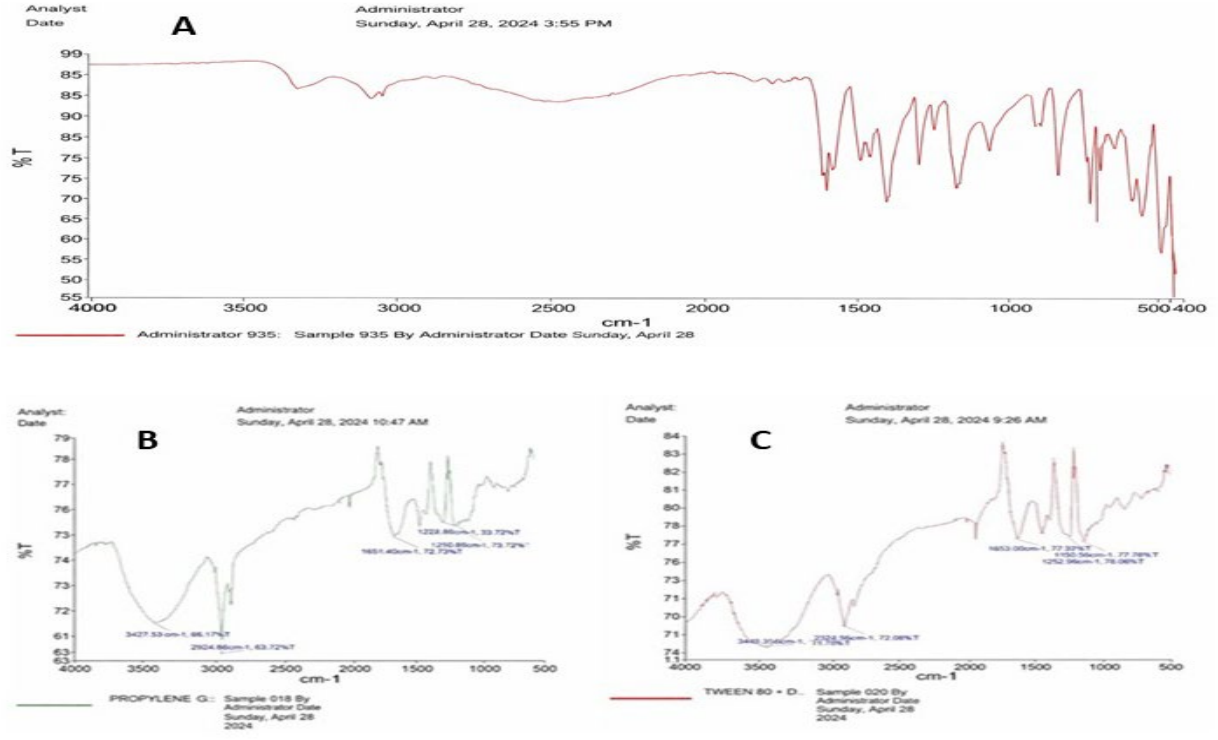

Figure 2. FTIR Spectrum A. Flucytosine (Pure drug), B. Flucytosine with Propylene Glycol and C. Flucytosine with Tween 80

X-ray diffraction (XRD) study

The XRD pattern of flucytosine (Figure 3) exhibits multiple sharp and intense diffraction peaks at specific 2θ values, indicating a well-defined crystalline structure. The presence of high-intensity, narrow peaks confirms the crystalline nature and long-range molecular order of the drug substance. No broad halos characteristic of amorphous material were observed, suggesting minimal or no amorphous content. The absence of extra or unidentified peaks in the diffractogram indicates that the sample is phase-pure and free from detectable crystalline impurities. Overall, the XRD results confirm that flucytosine exists predominantly in a crystalline form, which is important for its stability, reproducibility, and performance in pharmaceutical formulations.

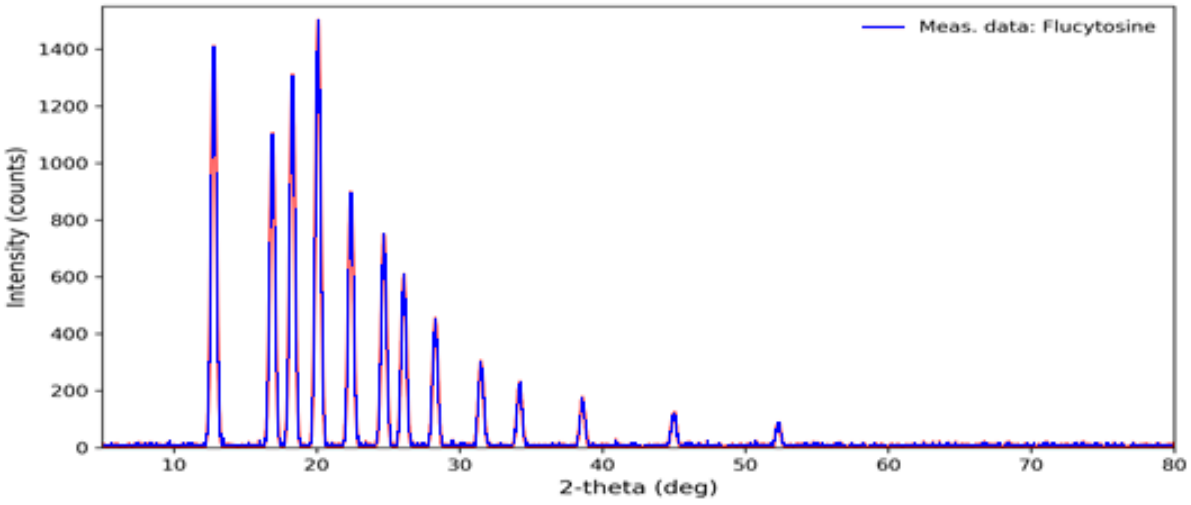

Figure 3. XRD of Flucytosine

Formulation Development and Optimization

Experimental Design Analysis

Seventeen nanoemulsion formulations were prepared according to the Box–Behnken design using three independent variables: lipid concentration (X_1), Smix ratio (X_2), and homogenization time (X_3). Particle size (Y_1), polydispersity index (Y_2), and entrapment efficiency (Y_3) were selected as dependent responses.

Quadratic models were found to best fit the experimental data for all responses. The coefficient of determination (R^2) values were 0.9727 for particle size, 0.9904 for PDI, and 0.9602 for entrapment efficiency, indicating excellent model fitting. Adequate precision values exceeded 4 for all responses, confirming model reliability.

Effect on Particle Size

The particle size of the flucytosine nanoemulsion was significantly affected by the studied variables, as evident from the 3D response surface and cube plots (Figure 4A and Table 2). Table 2 shows that all of the nanoemulsion formulations had tiny particle sizes. The following equation was produced using coded values:

$$Particle\ size = 420.875 - 21.925(X_1) + 15.25(X_2) - 5.00(X_3) + 0.900(X_1)(X_2) + 0.0400(X_1)(X_3) + 0.200(X_2)(X_3) + 0.6350(X_1)^2 - 12.500(X_2)^2 + 0.085(X_3)^2 \quad (1)$$

Due to improved interfacial stability and decreased interfacial tension, which promote effective droplet disintegration during homogenization, an increase in surfactant concentration resulted in a noticeable decrease in the particle size. Similar to this, longer homogenization times led to lower particle sizes because to cavitation effects and sustained shear stress, which encouraged the creation of finer droplets. On the other hand, higher oil concentration increased particle size, perhaps as a result of droplet coalescence brought on by inadequate surfactant coverage at high oil levels. Extended homogenization might partially counterbalance the size-increasing effect of increased oil content, but it could not completely counteract it, according to the interplay between oil concentration and homogenization time. Overall, the DOE found an ideal area, where nanoemulsions with the smallest particle size, suitable for improved stability and drug delivery performance, were created by low oil content, high surfactant concentration, and extended homogenization duration.

Effect on Polydispersity Index (PDI)

The polydispersity index of the synthesized flucytosine loaded nanoemulsion is indicated in Table 2. Table 2 shows that every nanoemulsion formulation had a low polydispersity index (PDI). The effects of amount of oil (X1), Smix (X2), and homogenization time (X3) on PDI (X1), Smix (X2), and homogenization time (X3) on the PDI is illustrated by the response surface and cube plots in Figure 4B. The following was the final equation in terms of coded values:

$$PDI = 0.2157 - 0.0119(X_1) - 0.1195(X_2) + 0.0043(X_3) - 0.0008(X_1)(X_2) - 0.00004(X_1)(X_3) + 0.003(X_2)(X_3) + 0.000506X_1)^2 + 0.0180(X_2)^2 - 0.00016(X_3)^2 \quad (2)$$

The response surface plots showed that as surfactant concentration and homogenization time increased, PDI decreased, suggesting the creation of more homogeneous nanoemulsions. PDI values were rather high at low surfactant levels, indicating a wider droplet size distribution and inadequate stability. By dissolving larger droplets and reducing aggregation, longer homogenization times

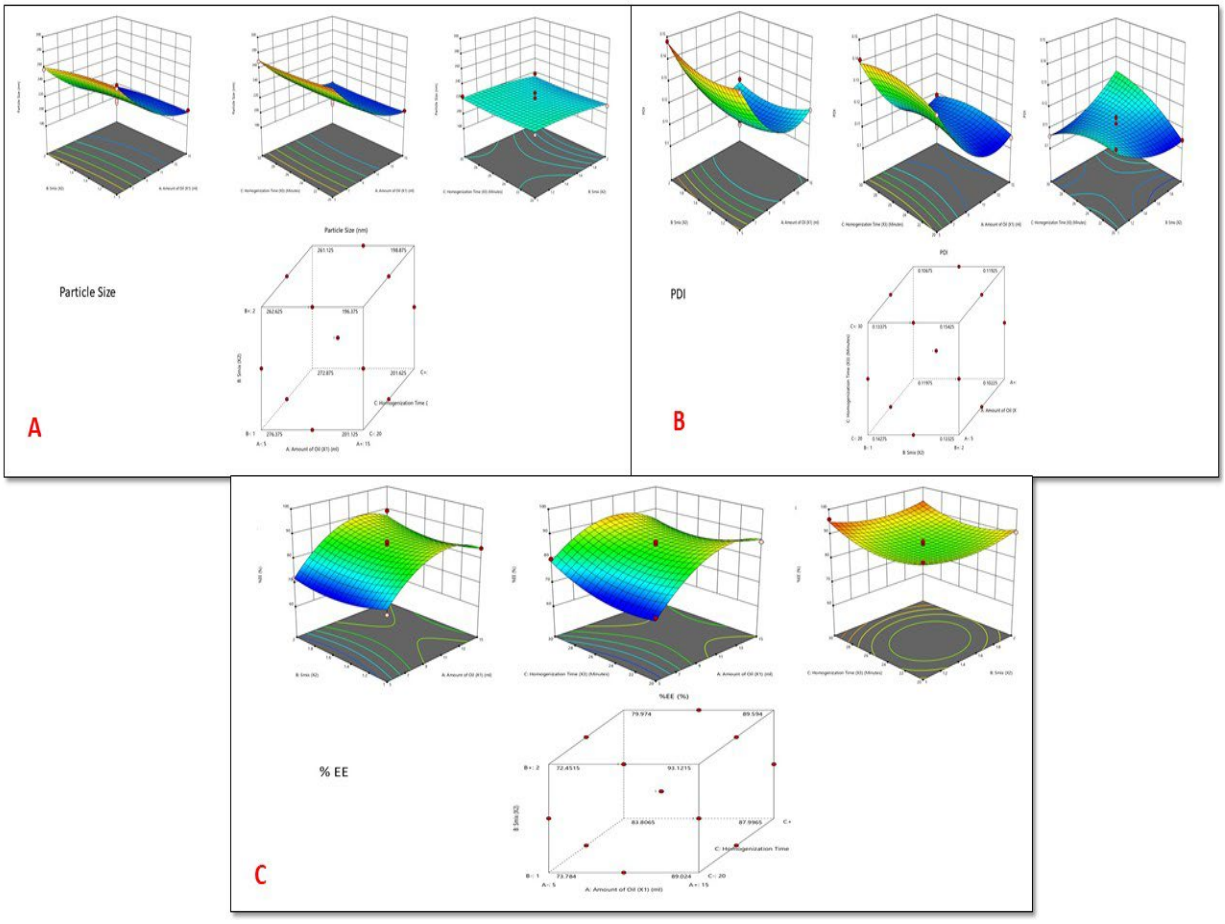

Figure 4. (A) Response 3D plots and Cube plots for the effect of amount of oil (X1), Smix(X2) and homogenization time (X3) on particle size, (B) Response 3D plots and Cube plots for the effect of amount of oil (X1), Smix(X2) and homogenization time (X3) on PDI, and (C) Response 3D plots and Cube plots for the effect of amount of oil (X1), Smix(X2) and homogenization time (X3) on % EE

increased size uniformity. Particularly when paired with shorter homogenization periods, higher oil concentrations marginally raised PDI, indicating that extra oil encourages heterogeneity if it is not sufficiently stabilized. Higher surfactant levels and prolonged homogenization were associated with the lowest PDI values (<0.3), indicating the creation of monodisperse and physically stable nanoemulsions.

Effect on % Entrapment Efficiency (%EE)

Table 2 displays the prepared flucytosine-loaded nanoemulsion's percentage EE. Every nanoemulsion formulation's %EE revealed a high % EE (Table 2). Figure 4C shows the cube plots and response surface for the impacts of homogenization time (X3), Smix (X2), and amount of oil (X1) on the % EE. In terms of coded values, the resulting equation was as follows:

$$\%\,EE = 134.1165 + 10.4358(X_1) - 36.3855(X_2) - 6.7182(X_3) + 0.5430(X_1)(X_2) - 0.1105(X_1)(X_3) - 0.2500(X_2)(X_3) - 0.3622(X_1)^2 + 12.4460(X_2)^2 + 0.1704(X_3)^2 \quad (3)$$

Response surface analysis revealed that increasing the oil concentration resulted in higher entrapment efficiency (%EE), owing to the increased internal phase volume available for drug solubilisation and retention. Additionally, moderate to high surfactant concentration further improved %EE by enhancing oil droplet stability and reducing drug diffusion into the aqueous phase. However, a slight decrease in %EE was observed at very high surfactant levels, which may have been caused by greater drug partitioning into the external phase. The effect of homogenization time on % EE was moderately beneficial. While stable droplets created by adequate homogenization enhanced drug encapsulation, overly lengthy processing may encourage drug diffusion out of the oil phase, somewhat decreasing entrapment efficiency. In order to achieve high drug loading without sacrificing nanoemulsion stability, the ideal region for greatest % EE correlated with greater oil content, appropriate surfactant concentration, and controlled homogenization time.

Characterization of Nanoemulsion

Particle Size Distribution

The particle size analysis of flucytosine nanoemulsions (F1–F9) demonstrated mean droplet sizes in the range of 104.3 ± 1.9 nm to 154.7 ± 3.2 nm, confirming the successful development of nano-sized emulsions. A gradual decrease in particle size from F1 to F7 was observed, attributed to the optimized surfactant–co-surfactant ratio that improved interfacial stabilization and minimized droplet coalescence. Formulation F7 showed the smallest particle size along with the lowest PDI value (0.15 ± 0.01), indicating a narrow size distribution and superior formulation uniformity. In contrast, the higher PDI values of F1–F3 reflected broader size distributions, while the slight increase in particle size observed in F8 and F9 may be due to excessive surfactant concentration causing droplet aggregation or system saturation. Overall, the combined particle size and PDI findings identify F7 as the most optimized nanoemulsion, offering enhanced physical stability and potential for improved drug delivery performance.

Zeta Potential

The zeta potential values (Table 3) of the flucytosine nanoemulsions ranged from −14.2 ± 1.3 mV (F1) to −31.5 ± 1.1 mV (F9), indicating that all formulations possessed a negative surface charge. A progressive increase in the magnitude of negative zeta potential was observed from F1 to F9, which can be attributed to the increasing concentration of surfactant–co-surfactant system and improved interfacial stabilization. Formulations F6 to F9 exhibited zeta potential values greater than −25 mV, suggesting enhanced electrostatic repulsion between droplets and, consequently, improved physical stability against aggregation. Among all formulations, F7 demonstrated an optimal balance with a sufficiently high negative zeta potential (−27.6 ± 1.2 mV) along with the smallest particle size and lowest PDI, indicating a stable and uniformly dispersed nanoemulsion system. Overall, the zeta potential results confirm that increasing surfactant concentration improves droplet surface charge and stability, and the negative zeta potential values obtained are adequate to ensure colloidal stability of the flucytosine nanoemulsions.

pH and Conductivity Determination

The pH values of all nanoemulsion formulations ranged from 6.41 ± 0.04 to 6.88 ± 0.02, which are close to the physiological skin pH, indicating that the formulations are suitable for consider topical administration unless mucosal application was specifically investigated with minimal risk of irritation (Table 3).

Entrapment Efficiency (%EE)

The entrapment efficiency showed a marked improvement from 60.8 ± 2.3% (F1) to 94.8 ± 1.1% (F7), followed by a slight decline in F8 and F9. This increase in %EE can be attributed to reduced droplet size and optimized surfactant–co-surfactant ratios, which enhance drug solubilization within the nanoemulsion droplets. The marginal decrease at higher surfactant levels may be due to drug partitioning into the external aqueous phase. Overall, F7 demonstrated the highest entrapment efficiency, indicating optimal formulation composition, as shown in Table 3.

Table 3. Characterization Parameters of Flucytosine Nanoemulsions

Formulation	Zeta Potential (mV)	pH	Drug Content
F1	−14.2 ± 1.3	6.41 ± 0.04	91.2 ± 1.5
F2	−16.1 ± 1.4	6.46 ± 0.03	92.6 ± 1.4
F3	−17.8 ± 1.2	6.52 ± 0.02	93.8 ± 1.3
F4	−19.6 ± 1.3	6.58 ± 0.03	95.1 ± 1.2
F5	−21.4 ± 1.1	6.63 ± 0.02	96.4 ± 1.1
F6	−23.1 ± 1.4	6.69 ± 0.03	97.6 ± 1.0
F7	**−27.6 ± 1.2**	**6.75 ± 0.02**	**98.5 ± 0.8**
F8	−29.1 ± 1.3	6.82 ± 0.03	97.0 ± 0.7
F9	−31.5 ± 1.1	6.88 ± 0.02	96.3 ± 0.6

Values are expressed as mean ± SD (n = 3).

Drug Content

Drug content across all formulations remained high, ranging from 91.2 ± 1.5% to 98.5 ± 0.8%, confirming uniform drug distribution and minimal drug loss during formulation. A progressive increase in drug content was observed from F1 to F7, corresponding with improved formulation homogeneity and stability. Slight reductions in F8 and F9 may be related to increased system viscosity or phase distribution effects. The consistently high drug content values demonstrate good reproducibility and reliability of the nanoemulsion preparation method, as shown in Table 3.

Morphology study by TEM

The structural characteristics of the optimized flucytosine nanoemulsion (F7) (Figure 5) were examined using transmission electron microscopy (TEM). The globules were spherical in shape and had an average diameter between 100 and 200 nm, which is consistent with the expected design. The nanoemulsion's homogeneous dispersion ensures consistent release patterns and bioavailability, supporting reliable drug delivery. The majority of the particles were smaller than 200 nm, which may improve the therapeutic efficacy of flucytosine by increasing its solubility and rate of dissolution. Because of its better permeability and retention as well as its predictable release profile, spherical shapes are preferred in drug delivery devices.

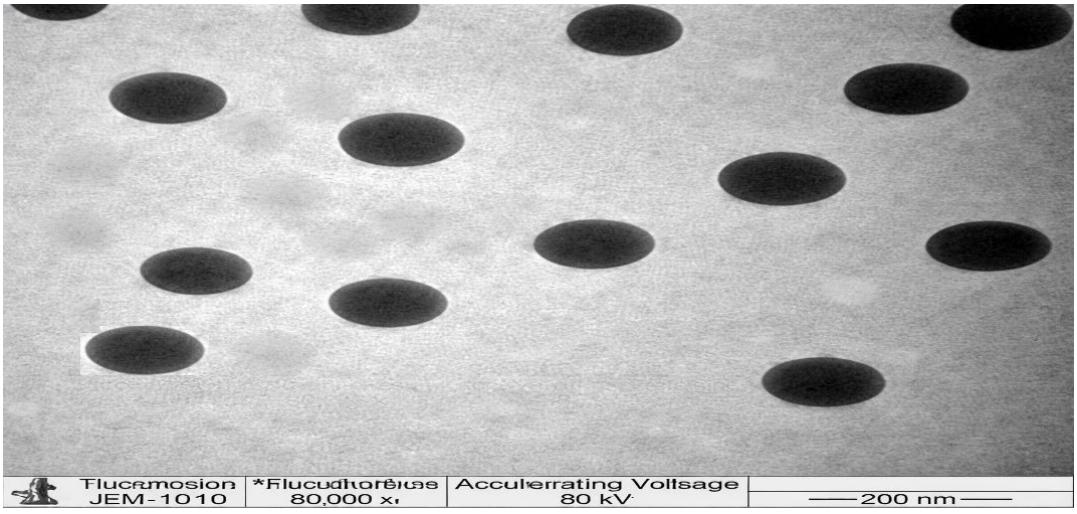

Figure 5. TEM of Optimized Flucytosine Nanoemulsion (F7)

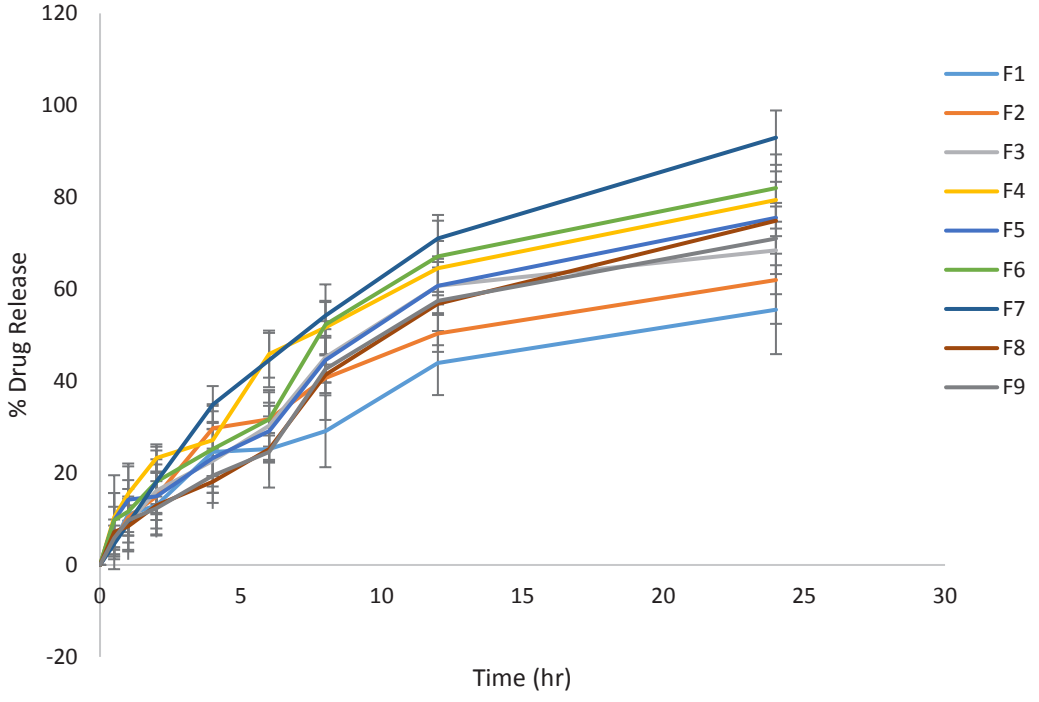

Figure 6. In-vitro drug release profile of various batches of nanoemulsion formulations

In Vitro drug release

Flucytosine nanoemulsions (F1–F9) showed a time-dependent and sustained release pattern over a 24-hour period in the in vitro drug release study. Flucytosine's regulated diffusion from the nanoemulsion system was demonstrated by all formulations' limited drug release at the initial time point, which was followed by a slow rise. The presence of surface-associated drug may be responsible for the first moderate burst release seen in the first one to two hours, whereas diffusion from the inside oil droplets is reflected in the sustained release phase that follows. F7 was the formulation with the greatest cumulative drug release (92.97 ± 5.91% at 24 hours), followed by F6 (82.00 ± 7.32%) and F4 (79.41 ± 6.22%). F7's smaller particle size, lower PDI, greater entrapment efficiency, and ideal surfactant–co-surfactant ratio, all of which increase surface area and facilitate effective drug diffusion, can be linked to its improved release. Formulations F1–F3 had somewhat reduced drug release, which might be the result of slower drug diffusion brought on by bigger droplet size and decreased entrapment efficiency. Overall, the findings show that the release behavior of flucytosine

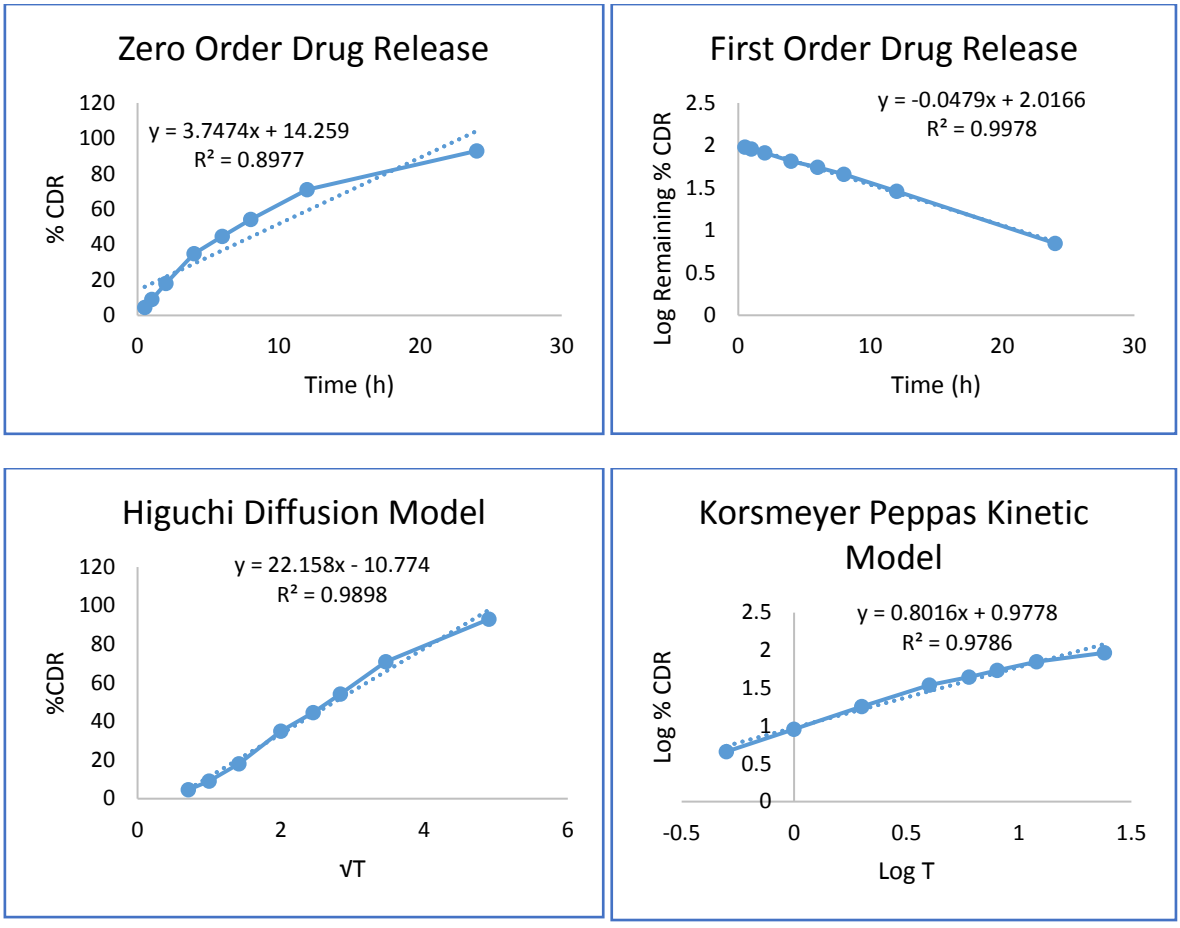

Figure 7. In-vitro drug release kinetics of Optimized Flucytosine nanoemulsion

nanoemulsions is strongly influenced by the formulation composition. The optimized formulation F7 showed better and prolonged drug release, demonstrating its potential as an effective nanoemulsion system for enhanced flucytosine delivery, as illustrated in Figure 6.

Release Kinetics

In vitro release data were subjected to several kinetic models, including the Zero-order release kinetics model, First-order release kinetics model, Higuchi diffusion model, and Korsmeyer–Peppas kinetic model. The regression coefficient (r) for all kinetic models are included in the Table 4 for the nanoemulsion formulation F7. The plots are displayed in the Figure 7. The elevated degree of the correlation coefficient identifies the appropriate kinetic model governing drug release kinetics from the aforementioned table; it was observed that first-order kinetics exhibited the highest correlation coefficient compared to other kinetic models.

Table 4. Coefficient of determination (R^2) values for different kinetic models for the optimized flucytosine nanoemulsion formulation (F7)

Kinetic Model	Coefficient of determination (R^2)
Zero Order	0.8977
Frist Order	0.9978
Higuchi Model	0.9898
Korsmeyer-Peppas	0.9786

Table 5. Antifungal Activity of Flucytosine Nanoemulsion by Zone of Inhibition

Sample	Zone of Inhibition (mm)
Flucytosine Solution	14.2 ± 0.8
Flucytosine Nanoemulsion (F7)	22.6 ± 1.1
Blank Nanoemulsion	No zone
Standard Antifungal (Fluconazole)	24.1 ± 0.9

Table 6. Stability studies result of optimized formulation (F7)

Storage Condition	Time (Months)	Appearance	Particle Size (nm)	PDI	Zeta Potential (mV)	pH	% EE	Drug Content (%)
Initial	0	Clear, homogeneous	104.3 ± 1.9	0.15 ± 0.01	−27.6 ± 1.2	6.75 ± 0.02	94.8 ± 1.1	98.5 ± 0.8
4 ± 2 °C	1	No change	105.1 ± 2.1	0.16 ± 0.01	−27.2 ± 1.3	6.74 ± 0.03	94.2 ± 1.2	98.1 ± 0.9
	2	No change	106.4 ± 2.3	0.17 ± 0.02	−26.9 ± 1.4	6.73 ± 0.03	93.6 ± 1.4	97.8 ± 1.0
	3	No change	107.2 ± 2.5	0.18 ± 0.02	−26.5 ± 1.5	6.72 ± 0.04	92.9 ± 1.6	97.4 ± 1.1
25 ± 2 °C / 60 ± 5% RH	1	No change	106.3 ± 2.4	0.17 ± 0.01	−26.8 ± 1.3	6.73 ± 0.03	93.8 ± 1.3	97.9 ± 0.9
	2	No change	108.5 ± 2.6	0.18 ± 0.02	−26.2 ± 1.4	6.71 ± 0.04	92.7 ± 1.5	97.2 ± 1.1
	3	No change	110.2 ± 2.9	0.19 ± 0.02	−25.6 ± 1.6	6.69 ± 0.05	91.8 ± 1.7	96.6 ± 1.2
40 ± 2 °C / 75 ± 5% RH	1	No change	109.6 ± 2.8	0.19 ± 0.02	−25.9 ± 1.4	6.70 ± 0.04	92.4 ± 1.6	96.9 ± 1.2
	2	Slight turbidity	112.8 ± 3.1	0.21 ± 0.02	−25.1 ± 1.6	6.68 ± 0.05	91.2 ± 1.8	96.1 ± 1.3
	3	Slight turbidity	116.5 ± 3.4	0.23 ± 0.03	−24.3 ± 1.7	6.65 ± 0.06	89.7 ± 2.0	95.4 ± 1.5

Antifungal Activity by Zone of Inhibition

The agar well diffusion technique was used to assess the flucytosine nanoemulsion's antifungal efficacy against *Candida albicans*. A distinct and well-defined zone of inhibition surrounding the wells was created by the flucytosine nanoemulsion, demonstrating strong antifungal action. By contrast, the blank nanoemulsion had no inhibitory zone and the plain flucytosine solution had a much smaller zone of inhibition, indicating that the drug's presence alone was responsible for the antifungal action. The nanoemulsion formulation's nanoscale droplet size, which enhances drug solubility, diffusion, and contact with the fungal cell membrane, is responsible for the increased zone of inhibition seen. Surfactants and co-surfactants may help drugs enter fungal cells more easily, increasing the effectiveness of antifungals. Overall, the findings show that the flucytosine nanoemulsion has better antifungal efficacy against *Candida albicans* than the traditional drug solution, underscoring its promise as an efficient antifungal therapeutic delivery method, as shown in Table 5.

Stability studies

Over a 3-month period, the improved flucytosine nanoemulsion demonstrated high physical and chemical stability under ambient temperature, refrigeration, and rapid storage. Phase separation, creaming, and cracking did not occur in the formulation; only a little amount of turbidity was noticed later on under accelerated circumstances. Higher temperatures and longer storage times were associated with slight increases in particle size and PDI, although these changes were within reasonable bounds. Maintained electrostatic stability and physiological compatibility were shown by the little changes in pH and zeta potential. Drug content and entrapment efficiency only marginally declined, staying within acceptable bounds. Overall, the findings support the stability and suitability of the flucytosine nanoemulsion for additional pharmaceutical development, as shown in Table 6.

Conclusion

To improve the drug's distribution and antifungal effectiveness, flucytosine nanoemulsions were effectively created using the Box–Behnken design approach to enhance its physicochemical characteristics, stability, and antifungal efficacy. Flucytosine's purity and compatibility with particular excipients were verified by preformulation and compatibility tests. Among the developed formulations, the optimized nanoemulsion F7, composed of liquid paraffin (oil phase), Tween-80, and propylene glycol as the surfactant–co-surfactant mixture (S_{mix}), distilled water as the aqueous phase, and flucytosine (100 mg), exhibited the most desirable characteristics. The optimized component ratio produced nano-sized droplets with low polydispersity, high entrapment efficiency, and improved antifungal activity, demonstrating the effectiveness of the selected formulation composition for enhanced drug delivery. When compared to other formulations, the optimized nanoemulsion demonstrated a prolonged and noticeably better in vitro drug release. A greater zone of inhibition compared to the ordinary medication

solution indicated improved therapeutic effectiveness and enhanced antifungal activity against *Candida albicans*. The improved formulation remained chemically and physically stable across a variety of storage settings, according to stability experiments. All things considered, the flucytosine nanoemulsion is a reliable and efficient delivery method for enhancing antifungal treatment and warrants further in vivo and clinical investigations to establish its therapeutic applicability.

AUTHOR CONTRIBUTIONS

All authors made substantial contributions to conception and design, acquisition of data, or analysis and interpretation of data; took part in drafting the article or revising it critically for important intellectual content; agreed to submit to the current journal; gave final approval of the version to be published; and agree to be accountable for all aspects of the work. All the authors are eligible to be an author as per the European Pharmaceutical Journal requirements/guidelines.

CONFLICTS OF INTEREST

The authors report no financial or any other conflicts of interest in this work.

DATA AVAILABILITY

All data generated and analyzed are included in this research article.

References

[1] Ali, A., Chiang, Y. W., & Santos, R. M. (2022). X-ray diffraction techniques for mineral characterization: A review for engineers of the fundamentals, applications, and research directions. *Minerals*, *12*(2), 205. https://doi.org/https://doi.org/10.3390/min12020205

[2] Anwer, M. K., Aldawsari, M. F., Iqbal, M., Almutairy, B. K., Soliman, G. A., & Aboudzadeh, M. A. (2023). Diosmin-loaded nanoemulsion-based gel formulation: Development, optimization, wound healing and anti-inflammatory studies. *Gels*, *9*(2), 95. https://doi.org/10.3390/gels9020095

[3] Beg, S., Swain, S., Singh, H. P., Patra, C. N., & Rao, M. E. B. (2012). Development, optimization, and characterization of solid self-nanoemulsifying drug delivery systems of valsartan using porous carriers. *Aaps Pharmscitech*, *13*, 1416–1427.

[4] Clapham, D., Belissa, E., Inghelbrecht, S., Pensé-Lhéritier, A.-M., Ruiz, F., Sheehan, L., Shine, M., Vallet, T., Walsh, J., & Tuleu, C. (2023). A guide to best practice in sensory analysis of pharmaceutical formulations. *Pharmaceutics*, *15*(9), 2319. https://doi.org/10.3390/pharmaceutics15092319

[5] Cong, Y., Du, C., Wang, M., Jiang, Z., & Wang, M. (2021). Solubility of 5-fluorocytosine in different pure and binary mixed solvents: measurement, model correlation, solvent effect, and preferential solvation. *Journal of Chemical & Engineering Data*, *66*(8), 3090–3100. https://doi.org/https://doi.org/10.1021/acs.jced.1c00206

[6] Delma, F. Z., Al-Hatmi, A. M. S., Brüggemann, R. J. M., Melchers, W. J. G., de Hoog, S., Verweij, P. E., & Buil, J. B. (2021). Molecular mechanisms of 5-fluorocytosine resistance in yeasts and filamentous fungi. *Journal of Fungi*, *7*(11), 909. https://doi.org/10.3390/jof7110909

[7] Denning, D. W. (2024). Global incidence and mortality of severe fungal disease. *The Lancet Infectious Diseases*, *24*(7), e428–e438. https://doi.org/10.1016/S1473-3099(23)00692-8

[8] Goyal, G., Garg, T., Malik, B., Chauhan, G., Rath, G., & Goyal, A. K. (2015). Development and characterization of niosomal gel for topical delivery of benzoyl peroxide. *Drug Delivery*, *22*(8), 1027–1042. https://doi.org/10.3109/10717544.2013.855277

[9] Hurt, W. J., Harrison, T. S., Molloy, S. F., & Bicanic, T. A. (2021). Combination therapy for HIV-associated cryptococcal meningitis—a success story. *Journal of Fungi*, *7*(12), 1098. https://doi.org/10.3390/jof7121098

[10] Jacob, S., Kather, F. S., Boddu, S. H. S., Shah, J., & Nair, A. B. (2024). Innovations in nanoemulsion technology: enhancing drug delivery for oral, parenteral, and ophthalmic applications. *Pharmaceutics*, *16*(10), 1333. https://doi.org/10.3390/pharmaceutics16101333

[11] Jarvis, J. N., Lawrence, D. S., Meya, D. B., Kagimu, E., Kasibante, J., Mpoza, E., Rutakingirwa, M. K., Ssebambulidde, K., Tugume, L., & Rhein, J. (2022). Single-dose liposomal amphotericin B treatment for cryptococcal meningitis. *New England Journal of Medicine*, *386*(12), 1109–1120. https://doi.org/10.1056/NEJMc2206274

[12] Kamdi, D. B., Yerne, H. M., & Patil, S. R. (2020). Development and Validation of UV Spectroscopic Method for Estimation of Fluconazole in Tablet Dosage Form. *Am. J. PharmTech Res.*, *10*(01), 83–92. https://doi.org/10.46624/ajptr.2020.v10.i1.008

[13] Khani, S., Keyhanfar, F., & Amani, A. (2016). Design and evaluation of oral nanoemulsion drug delivery system of mebudipine. *Drug Delivery*, *23*(6), 2035–2043. https://doi.org/10.3109/10717544.2015.1088597

[14] Kumar, S., Ali, J., & Baboota, S. (2016). Design Expert® supported optimization and predictive analysis of selegiline nanoemulsion via the olfactory region with enhanced behavioural performance in Parkinson's disease. *Nanotechnology*, *27*(43), 435101. https://doi.org/10.1088/0957-4484/27/43/435101

[15] Linder, K. A., Kauffman, C. A., & Miceli, M. H. (2023). Blastomycosis: a review of mycological and clinical aspects. *Journal of Fungi*, *9*(1), 117. https://doi.org/10.3390/jof9010117

[16] Liu, D., Zhou, R., & Gao, X. (2025). Recent innovations and challenges in the treatment of fungal infections. *Frontiers in Cellular and Infection Microbiology*, *15*, 1676009. https://doi.org/10.3389/fcimb.2025.1676009

[17] McHale, T. C., Boulware, D. R., Kasibante, J., Ssebambulidde, K., Skipper, C. P., & Abassi, M. (2023). Diagnosis and management of cryptococcal meningitis in HIV-infected adults. *Clinical Microbiology Reviews*, *36*(4), e00156-22. https://doi.org/10.1128/cmr.00156-22

[18] Miot, J., Leong, T., Takuva, S., Parrish, A., & Dawood, H. (2021). Cost-effectiveness analysis of flucytosine as induction therapy in the treatment of cryptococcal meningitis in HIV-infected adults in South Africa. *BMC Health Services Research*, *21*, 1–11. https://doi.org/10.1186/s12913-021-06268-9

[19] Monograph, U. O. (2014). United States Pharmacopeial Convention. *Rockville, MD*, 3224.

[20] Nikolaev, B., Yakovleva, L., Fedorov, V., Li, H., Gao, H., & Shevtsov, M. (2023). Nano-and microemulsions in biomedicine: From theory to practice. *Pharmaceutics*, *15*(7), 1989. https://doi.org/10.3390/pharmaceutics15071989 Abstract

[21] Pangeni, R., Sharma, S., Mustafa, G., Ali, J., & Baboota, S. (2014). Vitamin E loaded resveratrol nanoemulsion for brain targeting for the treatment of Parkinson's disease by reducing oxidative stress. *Nanotechnology*, *25*(48), 485102. https://doi.org/10.1088/0957-4484/25/48/485102

[22] Patel, P., Ahir, K., Patel, V., Manani, L., & Patel, C. (2015). Drug-Excipient compatibility studies: First step for dosage form development. *The Pharma Innovation*, *4*(5, Part A), 14.

[23] Rai, M., Ingle, A. P., & Pandit, R. (2021). Nanoemulsions as antifungal agents: Mechanisms, efficacy, and future perspectives. *Journal of Applied Microbiology*, *131*(1), 3–18. https://doi.org/https://doi.org/10.1111/jam.14989

[24] Rampado, R., & Peer, D. (2023). Design of experiments in the optimization of nanoparticle-based drug delivery systems. *Journal of Controlled Release*, *358*, 398–419.

[25] Rasmussen, M. K., Pedersen, J. N., & Marie, R. (2020). Size and surface charge characterization of nanoparticles with a salt gradient. *Nature Communications*, *11*(1), 2337. https://doi.org/10.1038/s41467-020-15889-3

[26] Safhi, A. Y., Naveen, N. R., Rolla, K. J., Bhavani, P. D., Kurakula, M., Hosny, K. M., Abualsunun, W. A., Alissa, M., Alsalhi, A., & Alahmadi, A. A. (2023). Enhancement of antifungal activity and transdermal delivery of 5-flucytosine via tailored spanlastic nanovesicles: statistical optimization, in-vitro characterization, and in-vivo biodistribution study. *Frontiers in Pharmacology*, *14*, 1321517. https://doi.org/https://doi.org/10.3389/fphar.2023.1321517

[27] Sastré-Velásquez, L. E., Dallemulle, A., Kühbacher, A., Baldin, C., Alcazar-Fuoli, L., Niedrig, A., Müller, C., & Gsaller, F. (2022). The fungal expel of 5-fluorocytosine derived fluoropyrimidines mitigates its antifungal activity and generates a cytotoxic environment. *PLoS Pathogens*, *18*(12), e1011066.

[28] Shaker, D. S., Ishak, R. A. H., Ghoneim, A., & Elhuoni, M. A. (2019). Nanoemulsion: A review on mechanisms for the transdermal delivery of hydrophobic and hydrophilic drugs. *Scientia Pharmaceutica*, *87*(3), 17. https://doi.org/10.3390/scipharm87030017

[29] Shi, Y., Zhang, M., Chen, K., & Wang, M. (2022). Nanoemulsion prepared by high pressure homogenization method as a good carrier for Sichuan pepper essential oil: Preparation, stability, and bioactivity. *Lwt*, *154*, 112779. https://doi.org/10.1016/j.lwt.2021.112779

[30] Sigera, L. S. M., & Denning, D. W. (2023). Flucytosine and its clinical usage. *Therapeutic Advances in Infectious Disease*, *10*, 20499361231161388. https://doi.org/https://doi.org/10.1177/20499361231161

[31] Tayeb, H. H., Felimban, R., Almaghrabi, S., & Hasaballah, N. (2021). Nanoemulsions: Formulation, characterization, biological fate, and potential role against COVID-19 and other viral outbreaks. *Colloid and Interface Science Communications*, *45*, 100533. https://doi.org/10.1016/j.colcom.2021.100533

[32] Tkachenko, Y., & Niedzielski, P. (2022). FTIR as a method for qualitative assessment of solid samples in geochemical research: a review. *Molecules*, *27*(24), 8846. https://doi.org/https://doi.org/10.3390/molecules27248846

[33] Vishwas, S., Kumar, R., Awasthi, A., Corrie, L., Bashir, B., Khursheed, R., Ramanunny, A. K., Gulati, M., Singh, T. G., & Gupta, G. (2024). Formulation and optimization of fisetin nanoemulsion for the treatment of Alzheimer's disease in rats: Pharmacokinetic and pharmacodynamic assessment. *Journal of Drug Delivery Science and Technology*, *101*, 106269. https://doi.org/https://doi.org/10.1016/j.jddst.2024.106269

[34] Yalkowsky, S. H., & Alantary, D. (2018). Estimation of melting points of organics. *Journal of Pharmaceutical Sciences*, *107*(5), 1211–1227. https://doi.org/10.1016/j.xphs.2017.12.013